Available online at www.sciencedirect.com
ScienceDirect
Bioelectrochemistry 70 (2007) 363–368
Bioelectrochemistry
www.elsevier.com/locate/bioelechem

# Using a micro electroporation chip to determine the optimal physical parameters in the uptake of biomolecules in HeLa cells

Huiqi He [a,c], Donald C. Chang [b], Yi-Kuen Lee [a,c,*]

[a] Bioengineering Graduate Program, Hong Kong University of Science and Technology, Clear Water Bay, Kowloon, Hong Kong SAR, China
[b] Department of Biology, Hong Kong University of Science and Technology, Clear Water Bay, Kowloon, Hong Kong SAR, China
[c] Department of Mechanical Engineering, Hong Kong University of Science and Technology, Clear Water Bay, Kowloon, Hong Kong SAR, China

Received 14 February 2006; received in revised form 6 April 2006; accepted 13 May 2006
Available online 23 May 2006

**Abstract**

In this study, a new micro electroporation (EP) cell chip with three-dimensional (3D) electrodes was fabricated by means of MEMS technology, and tested on cervical cancer (HeLa) cells. Extensive statistical data of the threshold electric field and pulse duration were determined to construct an EP "phase diagram", which delineates the boundaries for 1) effective EP of five different size molecules and 2) electric cell lysis at the single-cell level. In addition, these boundary curves (i.e., electric field versus pulse duration) were fitted successfully with an exponential function with three constants. We found that, when the molecular size increases, the corresponding electroporation boundary becomes closer to the electric cell lysis boundary. Based on more than 2000 single-cell measurements on five different size molecules, the critical size of molecule was found to be approximately 40 kDa. Comparing to the traditional instrument, MEMS-based micro electroporation chip can greatly shorten the experimental time.


*Keywords:* Micro electroporation; MEMS; 3D electrode; HeLa cells; Membrane permeability; Phase diagram; Size effect

## 1. Introduction

Electroporation (EP) is a widely-used technique for delivering a large variety of impermeable molecules, such as drugs, antibodies, oligonucleotides, RNA and DNA plasmids [1–5], the electric parameters for loading different molecules into different cells may vary significantly from one experiment to another. For instance, the pulse amplitude can range from 0.3 kV/cm to 12 kV/cm, and the pulse duration from 0.5 μs to 50 ms. Large molecules can penetrate cells only at high field strength or extended pulse length, when a population of larger size pores is created and the critical size of molecular weight is reported to be around 40 kDa [6]. The basic relationship between the parameters of major importance–field strength and pulse duration–initially was addressed by Dev et al. [7] to qualitatively describe the boundaries of electroporation and electric cell lysis. However, to date the optimal conditions for electroporating specific molecules into cells has not been well addressed.

In this paper, a new micro electroporation chip, based upon a modified electroplating technique, was designed and fabricated. It can be used to study the "phase diagram" of cervical cancer cells (HeLa cell line) for electroporating different size molecules. Using this design, large-scale EP experiments with different voltage, $U$, and pulse duration, $t_d$, can be conducted on a single chip at the same time.

## 2. Experimental studies

### 2.1. Device fabrication

A micro electroporation chip with twelve pairs of three-dimensional multiple input electrodes was fabricated on a glass

* Corresponding author. Department of Mechanical Engineering, HKUST, Clear Water Bay, Kowloon, Hong Kong. Tel.: +852 2358 8663; fax: +852 2358 1543.
*E-mail address:* meyklee@ust.hk (Y.-K. Lee).

1567-5394/$ - see front matter © 2006 Elsevier B.V. All rights reserved.
doi:10.1016/j.bioelechem.2006.05.008

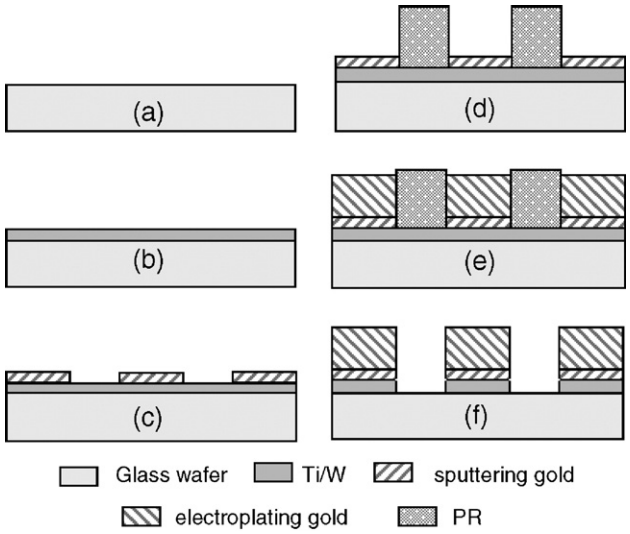


Fig. 1. Fabrication process flow diagram of a micro EP chip: (a) glass wafer Pyrex 7740, (b) sputter a layer of Ti/W, (c) pattern Au layer by lift-off, (d) pattern thick photoresist for electroplating, (e) electro-plating gold electrode, (f) remove PR and Ti/W.

wafer utilizing electroplating technology. The thickness of sputtered thin-film planar electrodes using sputtering technique is usually less than 0.5 μm. Therefore, as described in our previous work [8], it is very difficult to achieve a uniform distribution of the electric field across the cell chamber. The majority of the high electric field strength area is close to the surface of the micro electroporation chip, especially in the area between the two electrodes. Consequently, this creates a large number of pores located only around the bottom of the cells that fill in the cell chamber. However, some negatively-charged molecules, like DNA plasmid, cannot precipitate to the bottom of the chip. Therefore, transfection efficiency can be very low. Here, we developed a new micro electroporation chip that has a 3D gold electrode with a height that is comparable to the diameter of the cell.

A modified electroplating process was adopted to avoid damage to the gold structure during the wet-etching process in an iodide bath. The gold seed layer was patterned, first using the lift-off technique, so that no additional step for removing the gold was required after the electroplating process. This can protect the electroplated structure from being attacked, and ensures that it is consistent with the original design.

The microfabrication process is shown in Fig. 1, a layer of Ti/W (100 nm) was sputtered by means of a CVC 601 sputtering system, as the conductive layer for electroplating. Then, a 200 nm gold layer was patterned, using the standard lift-off process as the seed layer. This, was followed by building a 20-μm-thick AZ4903 photoresist mold on the wafer. The electroplating process ultimately was carried out in Neutronex 309 (Cookson Electronics, United Kingdom), an alkaline and non-cyanide plating solution, for about 2 h at a temperature of 55 °C. The deposit speed was about 0.25 μm/min at the optimal current density of 4 mA/cm$^2$. In the end, the photoresist and the Ti/W layer were removed using a photoresist-stripping reagent MS2001 and hydrogen peroxide.

Twelve pairs of commonly-grounded 3D electrodes with different inputs were fabricated on the glass wafer. Each segmented electrode was made of 100-nm-thick sputtered titanium, 200-nm-thick sputtered gold and 12-μm-thick electroplated gold with a width of 30 μm. The space between adjacent electrodes was 30 μm. With such a design, 12 groups of results with different electric pulse amplitudes and pulse duration can be obtained on a single chip at the same time.

After all the fabrication processes were complete, the wafer then was diced and packaged on a printed circuit board (PCB), using wire-bonding technology. A 1-mm-diameter hole was drilled on the PCB at the area of the chip, for optical detection, under an inverted fluorescence microscope (Olympus IX70, Japan). PDMS (Sylgard 184, Dow Corning, USA), a biocompatible polymer material, was coated on the wire-bonded site to protect the wire from possible breakage during the cleaning process. A photo of a packaged micro EP chip and the SEM close-up view of the fabricated 3D electrode structures are shown in Fig. 2.

### 2.2. Electric field simulation

Compared to the 2D planar electrode reported in our previous work [8], the 3D electrode can provide a more uniformly-distributed electric field for single-cell electroporation.

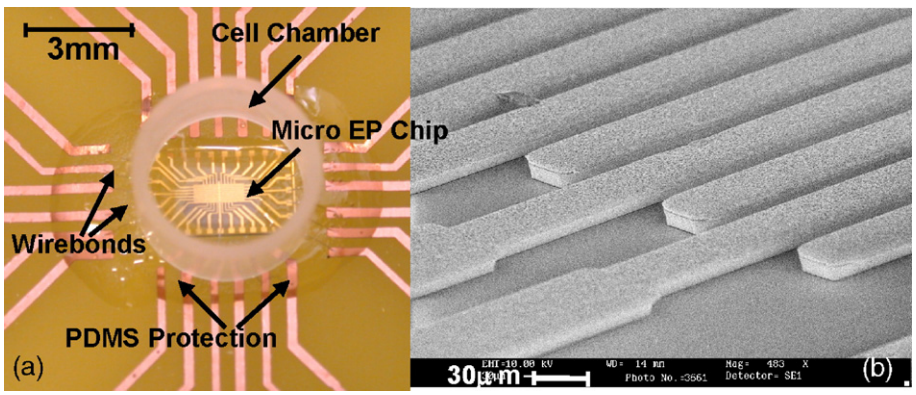


Fig. 2. (a) A photo of a packaged micro EP chip; (b) SEM close-up view of the 3D microelectrodes.

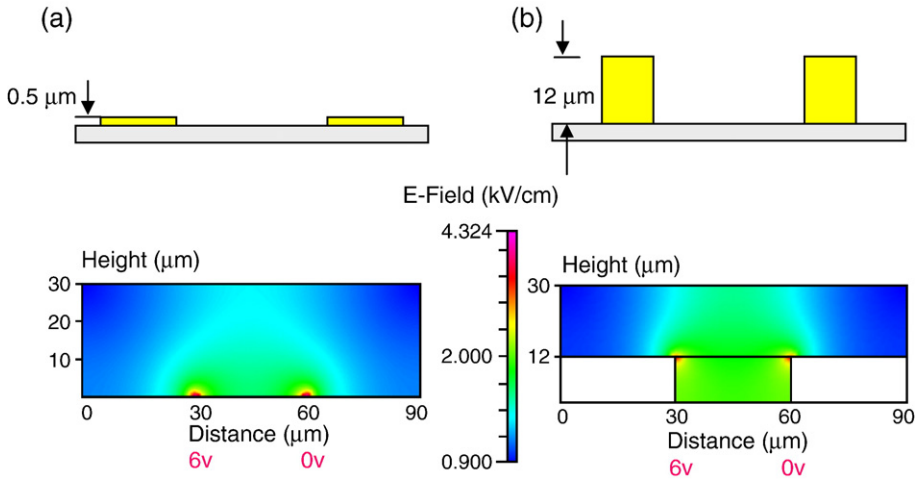


Fig. 3. Simulation results of the electric field distribution on a cross-section of 2D electrodes (a) and 3D electrodes (b).

The electric field distribution across the cell chamber for both 2D and 3D electrodes were simulated using commercial software (CFD-ACE+, ESI CFD Inc., AL, USA). A 2D simulation model was created, based upon the exact size of the chip with a mesh density of 90×30. The numerical model included two regions: gold electrodes and the region filled with poration media. The electric module in ACE was utilized and a fixed potential was defined as the boundary condition. Simulation results are demonstrated in Fig. 3. For 2D planar electrodes, most of the high electric field is close to the micro electroporation chip surface and concentrated between the two electrodes, while in other areas the electric field is much weaker. However, as shown in Fig. 3(b), with the 3D electrodes, the electric field distribution is much more uniform. Thus, a larger part of cell membranes can be exposed to the high electric field in this new design.

An estimate of the average electric field within the chip also can be obtained by averaging the non-uniform electric field distribution for each data point within the area of the electrodes. Therefore, the externally applied voltage $U_a$ can be converted to the average electric field $E_{avg}$ ($E_{avg}=\alpha U_a/L_e$, where $L_e$ is the distance between the two adjacent electrodes) via a correction factor ($\alpha_2=0.630$ for 2D electrode, $\alpha_3=0.976$ for 3D electrode) calculated from the numerical simulation. $L_e$ is 30 μm in this paper. Obviously, the correction factor, $\alpha_3$, for the 3D electrode is closer to 1 (for the ideally uniform electric field). Note that all the electric fields used in the rest of this paper are the average electric field calculated by the aforementioned equation.

### 2.3. Electric field pulse delivery

The pulsed radio-frequency (RF) electric field with adjustable frequency, amplitude and pulse duration was applied to the micro EP chip using a Labview program and the PCI 6110 DAQ card (National Instrument, TX, USA). The main advantage of using a pulsed RF electric field is that it can counterbalance the cells' size effect with an opposite effect of cell relaxation [9,10]. As a result, the viability and permeability of the electroporation can be improved, versus the traditional DC pulse or exponential decay pulse [9–11].

### 2.4. Cell preparation and fluorescent probe

HeLa cells were grown as a monolayer in a 60 mm petri dish in EMEM medium (CCL-2™, ATCC, VA, USA), supplemented with 10% fetal bovine serum (ATCC, VA, USA) at 37 °C and 5% $CO_2$. Cells were trypsinized by 0.05% trypsin/EDTA and then were washed twice with the poration medium (comprised of 280 mM mannitol, 5 mM sodium phosphate, 10 mM potassium phosphate, 1 mM $MgCl_2$ and 10 mM HEPES at the pH level of 7.4) by spinning at 1400 rpm at room temperature. Subsequently, they were re-suspended in the poration medium at a concentration of $5\times10^5$ cells/mL. The devices first were sterilized with 75% ethanol solution, rinsed with DI water and finally dried in a 65 °C oven.

To quantitatively detect the results of electroporation, a fluorescent dye, propidium iodide (PI) (P-4170, Sigma-Aldrich, MO, USA; molecular weight 668.4) was used in the experiments. PI dye is a membrane-impermeable nucleic acid intercalator that shows no auto-fluorescence, but it can become fluorescent when bound to nucleic acids with an excitation/emission maxima at 535/617 nm. Thus, the contrast is high between the cells uploaded with dye molecules and the background. This ensures good-quality fluorescence images being obtained. In the experiments, PI dye was dissolved in the cell suspension prior to electroporation, in order to achieve the desired concentration of 15 μg/mL.

Rhodamine B-labeled dextran (D-1824, Invitrogen), RITC-label dextran (R9006, Sigma-Aldrich) and FITC-labeled dextrans (FD-40S, FD-70S, Sigma-Aldrich) with average molecular weights of 10, 20, 40, 70 kDa were used as macromolecules with approximate physical diameters of 4.6 nm, 6.6 nm, 9 nm and 12 nm, respectively (product information data from Sigma-Aldrich). The concentrations of dextrans were adjusted to 0.4% (w/v).

## 3. Results and discussion

### 3.1. Electric field strength, pulse duration and pulse number

Cell permeabilization only can be detected if the applied electric field amplitude and pulse duration are higher than their thresholds. The uptake of PI was quantified by the associated fluorescence intensity, which reflects its free diffusion across the permeabilized cell membrane. Our micro EP chip can realize the large-scale cell-array that is crucial for a high-throughput *in situ* electroporation study. The variations in fluorescence intensity of the suspended HeLa cells, as a function of $U$ (or electric field strength, $E$) under different pulse durations, $t_d$, and different pulse number were measured and the results are shown in Fig. 4. It can be seen that increasing the pulse amplitude and duration both enhance cell uptake of fluorescent dye, while pulse amplitude plays a more important role comparing with the pulse duration. It is demonstrated in Fig. 4(b) that if the electric field is smaller than the critical value, extension of the pulse duration can not induce the electroporation. Only the pulse amplitude is above the critical electric field, nanometer-sized pores can be induced on the cell membrane and the dye molecules can diffuse into the cell through the pores, as shown in Fig. 4(a). The critical voltages are different for different pulse duration and in general, the critical voltage is lower for longer pulse duration. Moreover, further increase of the pulse amplitude does not increase the membrane permeability any more and the fluorescent intensity becomes stable. At this stage some cells can undergo lysis. Apart from the electric field amplitude and pulse duration, the pulse number also can affect the results of electroporation, Fig. 4(c) and (d) shows the uptake of PI dye as functions of pulse amplitude and pulse number, with 400 μs and 1 ms pulse duration, respectively. Increasing pulse number can enhance the uptake of molecules under the same pulse amplitude and pulse duration.

### 3.2. Loading different sizes of molecules

Different sizes of molecules, including Rhodamine B–dextran with a molecular weight of 10 kDa, RITC–dextran with a molecular weight of 20 kDa, FITC–dextran with a molecular weight of 40 kDa and 70 kDa, and a gene-coding green fluorescent protein, were introduced into HeLa cells, as shown in Fig. 5(a), (b), (c), (d) under a fluorescence field. For fluorescence-labeled dextran, 20 μL of the cell suspension with dextran was pipetted and loaded onto the micro EP chip. After the electric pulse treatment, 200 μL culture medium was added and cells remained on the chip for 4 h to attach to the chip. Cells then were rinsed with PBS 5 times to remove the additional fluorescence background, before examination under the microscope.

Fig. 5(e) shows the loading efficiency of five different molecules, as a function of the average electric field with a single pulse duration of 400 μs. For all these 5 molecules, the

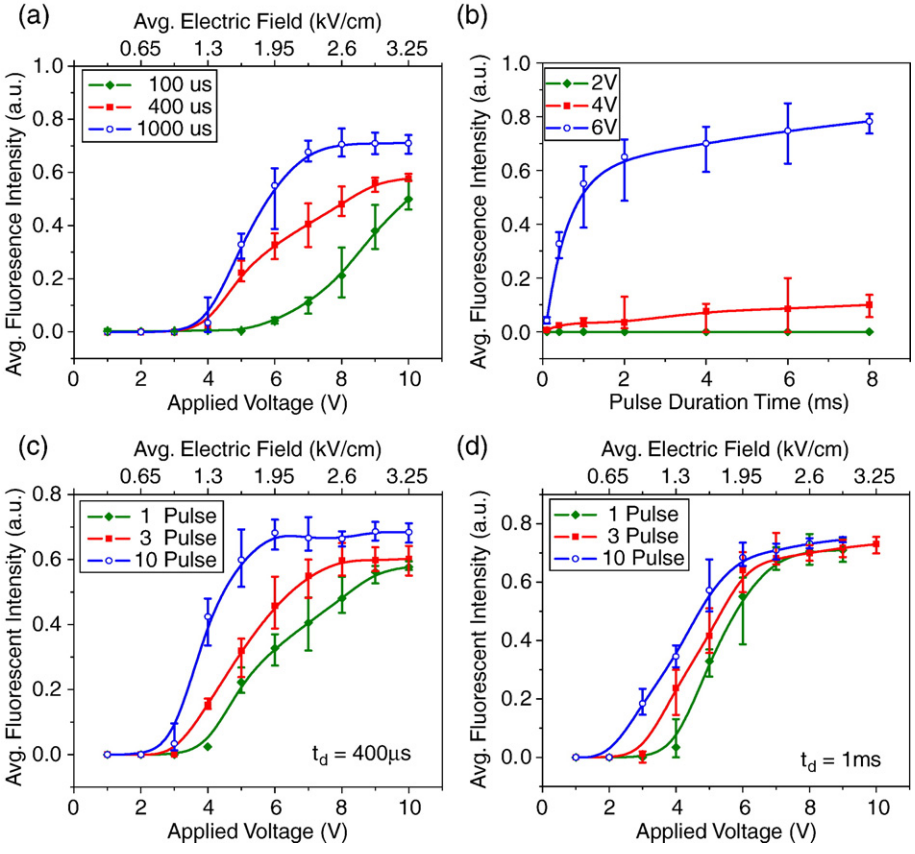


Fig. 4. Average fluorescence intensity as a function of applied voltage (a), pulse duration (b), and pulse number (c) and (d). Each data point from the average of 10 single HeLa cells.

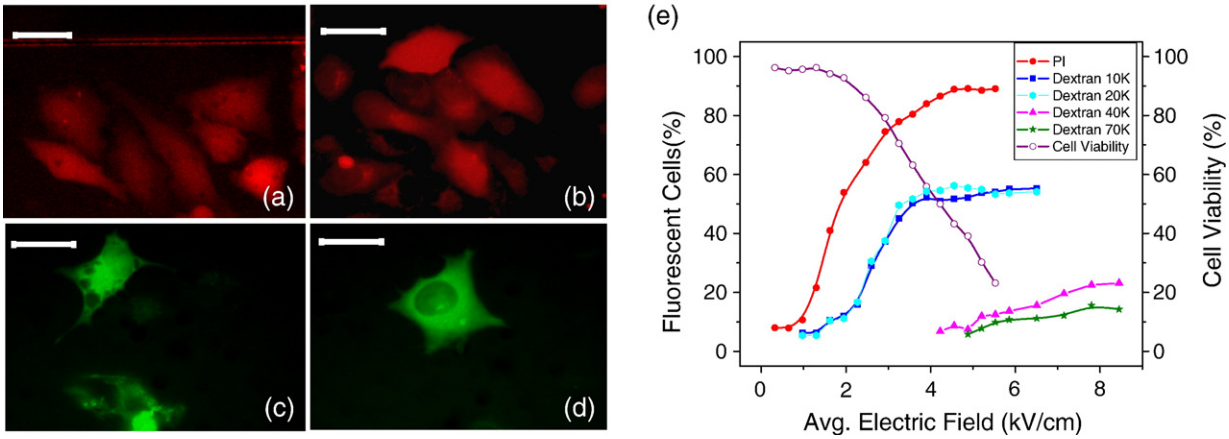


Fig. 5. Micrographs of HeLa cells after electroporation on micro EP chips, using 4 different macromolecules under fluorescence mode: (a) 10 kDa rhodamine B–dextran, (b) 20 kDa RITC–dextran, (c) 40 kDa FITC–dextran, and (d) 70 kDa FITC–dextran (all scale bars = 30 μm). (e) Loading efficiency of macromolecules with different molecular weights (pulse duration $t_d$ = 400 μs, single pulse).

loading efficiencies increased with an increase in the electric field. Conversely, cell viability decreased significantly with an increase in permeability. In addition, as shown in Fig. 5(e), the permeability of dextran during the micro electroporation process depends on its molecular weight. The higher the dextran's molecular weight, the lower its permeability was observed to be. This is due to the diameter of the pores, induced by external electric field, limiting the passage of dextran of a given size. This can be proven by the observation that large molecules can penetrate only at higher strength or increased pulse duration, which results in a population of larger size pores being created.

Furthermore, many of the conditions indicating uptake of large numbers of macromolecules are accompanied by a significant loss of cell viability. In addition, large molecules (40 kDa and 70 kDa dextran) cannot reach a penetration of 50% within such a short duration as 400 μs, while the viability already has dropped to lower than 20%. The results were consistent with Hui's conclusion [6], that there is a size cut-off criterion for dextran that falls somewhere between 9 kDa and 41 kDa, because dextran molecules with a molecular weight of 41 K or higher behave very differently from dextran with a molecular weight of 9 kDa. Based on what we obtained from the current study, it is now possible to narrow the critical size down to approximately 40 kDa (see Fig. 5).

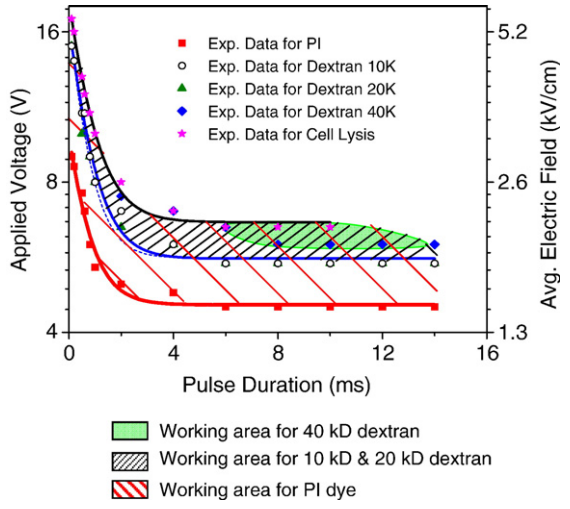


Fig. 6. The EP phase diagram for four different sizes of molecules. The threshold electric fields for loading different molecules ($E_{EP}$) and ECL ($E_{ECL}$) can be nicely fitted to exponential functions of $t_d$ (ms).

Quantitatively analysing 2000 data points, the critical voltage, $U$, for loading molecules of different sizes and Electric Cell Lysis (ECL) with different pulse durations, $t_d$, was determined, so as to construct the phase diagram shown in Fig. 6. Apparently, $U$ and $t_d$ can be traded off to a certain extent; i.e., lower $U$ needs longer $t_d$ to charge the cell membrane to reach the EP threshold voltage, $U_{EP}$. Conversely, if $U$ is high enough, it needs only a short $t_d$. However, treatment of cells with intense $U$ and short $t_d$ will lead to an irreversible process wherein the cell cannot repair the damage and will be lysed. On the other hand, cells can sustain a longer time period if a mild voltage is applied. In addition, larger molecule size results in narrower loading area at the same time that the boundary of electroporation becomes closer to the boundary of cell lysis. The boundary for loading 10 kDa dextran and 20 kDa dextran were almost overlapped, as the dash line shown in Fig. 6, while the boundary for loading 70 kDa dextran cannot be shown in the figure since the viability dropped to lower than 50% when loading efficiency reached 50%.

Table 1
The constants for the threshold electric field $E_{EP}-t_d$ relationship for four different molecules, Eq. (1)

| Molecules | $E_0$ | $E_1$ | $\tau$ (ms) | $R^2$ |
|---|---|---|---|---|
| PI dye | 1.464±0.2985 | 1.464 | 0.6932 | 0.9312 |
| 10 kDa dextran | 1.789±0.4648 | 3.0907 | 0.7478 | 0.9932 |
| 20 kDa dextran | 1.789±0.4834 | 3.0907 | 0.6404 | 0.9823 |
| 40 kDa dextran | 1.952±0.1240 | 0.7320 | 3.8825 | 0.9881 |

All the electric field constants are in kV/cm.

Moreover, the threshold electric fields, $E_{EP}$, for loading different molecules can be nicely fitted to an exponential function of pulse duration $t_d$ with three constants ($E_0$, $E_1$, $\tau$), as follows:

$$E_{EP} = E_0 + E_1 \exp(-t_d/\tau) \quad (1)$$

where $E_0$ is the electric field at the longest duration, $E_1$ is the difference of critical electric field at longest duration and shortest duration, $\tau$ (in ms) is the time constant of exponential decay curve. The error margins of the electric field based on 95% confidence interval are calculated and included in the constant $E_0$ [16]. All the coefficients of determination $R^2$ are higher than 0.93. All the constants and the error margins for the four different molecules are listed in Table 1.

In addition to the above curve fitting analysis, we found that the three constants in the exponential function can be simply determined from only three sets of experimental data points. The phase diagram was constructed from 2000 data points of single-cell electroporation measurements. Obviously, it was much more efficient and economic to obtain such a large-scale statistical data by using MEMS-based micro cell array chips in comparison with the micro electroporation chips reported in the literature [12–15].

## 4. Conclusions

A new micro electroporation chip with 12 groups of 3D electrodes has been designed and fabricated, using MEMS technology. We demonstrated that a large amount of statistical data for the electroporation of cervical cancer cells (HeLa cell line) at the single-cell level with different pulse amplitudes, pulse durations and pulse number can be obtained easily, so as to construct an EP phase diagram. The threshold electric field as a function of pulse duration for different size molecules can be nicely fitted into exponential functions. The electroporation phase diagram will be highly useful for electric parameter selection to improve the electroporation efficiency in future cell models.

## Acknowledgements

This work was supported by two Hong Kong Research Grants Council grants (Project Ref No. 616205 and HKUST6466/05M). The authors would like to thank Prof. Yitshak Zohar at University of Arizona, Tucson, USA, Ms. Vivian C. Yu, Ms. Inez Tsui, Mr. Wan Lap Yeung, Mr. Thomas W. H. Chau at HKUST for technical support.

## References

[1] D.C. Chang, J.A. Saunders, B.M. Chassy, A.E. Sowers, Overview of electroporation and electrofusion, in: D.C. Chang, J.A. Saunders, B.M. Chassy, A.E. Sowers (Eds.), Guide to Electroporation and Electrofusion, Academic Press, San Diego, 1992, pp. 1–6.
[2] J. Gehl, T. Skovsgaard, L.M. Mir, Enhancement of cytotoxicity by electropermeabilization : an improved method for screening drugs, Anti-Cancer Drugs (1998) 319–325.
[3] Y. Mouneimne, P.-F. Tosi, R. Barhoumi, C. Nicolau, Electroinsertion: an electrical method for protein implantation into cell membranes, in: D.C. Chang, J.A. Saunders, B.M. Chassy, A.E. Sowers (Eds.), Guide to Electroporation and Electrofusion, Academic Press, San Diego, 1992, pp. 1–6.
[4] L.M. Mir, H. Banoun, C. Paoletti, Introduction of definite amounts of nonpermeant molecules into living cells after electropermeabilization: direct access to the cytosol, Exp. Cell Res. 175 (1) (1988) 15–25.
[5] E. Neumann, M. Schaefer-Ridder, Y. Wang, Gene transfer into mouse lyoma cells by electroporation in high electric fields, EMBO J. 1 (1982) 541–845.
[6] H. Liang, W.J. Purucker, D.A. Stenger, R.T. Kubiniec, S.W. Hui, Uptake of fluorescence-labeled dextrans by 10T 1/2 fibroblasts following permeation by rectangular and exponential-decay electric field pulses, BioTechniques 6 (1998) 550–558.
[7] S.B. Dev, D.P. Rabussay, G. Widera, G.A. Hofmann, Medical applications of electroporation, IEEE T Plasma Sci. 28 (2000) 206–223.
[8] H. He, D.C. Chang, Y.-K. Lee, Micro pulsed radio-frequency electroporation chip, Bioelectrochemistry 68 (2005) 91–99.
[9] D.C. Chang, Cell poration and cell fusion using an oscillating electric field, Biophys. J. 56 (1989) 641–652.
[10] D.C. Chang, P.Q. Gao, B.L. Maxwell, High efficiency gene transfection by electroporation using a radio-frequency electric field, Biochim. Biophys. Acta 1092 (1991) 153–160.
[11] D.C. Chang, J.R. Hunt, Q. Zheng, P.-Q. Gao, Electroporation and electrofusion using a pulsed radio-frequency electric field, in: D.C. Chang, B.M. Chassy, J.A. Saunders, A.E. Sowers (Eds.), Guide to Electroporation and Electrofusion, Academic Press, San Diego, 1992, pp. 303–326.
[12] Y.-C. Lin, M.-Y. Huang, Electroporation microchips for in vitro gene transfection, J. Micromechanics Microengineering 11 (2001) 542–547.
[13] Y. Huang, B. Rubinsky, Microfabricated electroporation chip for single cell membrane permeabilization, Sens. Actuators, A, Phys. 89 (2001) 242–249.
[14] M. Khine, A. Lau, C. Ionescu-Zanetti, J. Seo, L.P. Lee, A single cell electroporation chip, Lab Chip 5 (2005) 38–43.
[15] Y.S. Shin, K. Cho, J.K. Kim, S.H. Lim, C.H. Park, K.B. Lee, Y. Park, C. Chung, D.C. Han, J.K. Chang, Electrotransfection of mammalian cells using microchannel-type electroporation chip, Anal. Chem. 76 (2004) 7045–7052.
[16] J.S. Milton, J.C. Arnold, Probability and Statistics in the Engineering and Computing Sciences, McGraw-Hill, New York, 1986.